Computational methods for symmetry-protected topological invariants

Tony Metger
Supervisor: Dominik Gresch

December 21, 2017

Abstract

Topological phases are novel quantum states of matter whose properties are closely related to the topology of the band structure. The topology of the band structure is robust to experimental noise, which makes these states useful for practical applications. Recently, numerical methods for identifying topological phases have been developed and implemented in the software package Z2Pack [1]. These methods rely on tracking the sum of Wannier charge centers of hybrid Wannier functions. In this work, we extend this numerical technique to symmetry-protected topological invariants. An implementation of this technique is provided in Z2Pack and tested for the Haldane model.

Contents

1 Introduction

Phases of matter and transitions between them are described by order parameters. In Landau's theory of phases, an order parameter is a quantity which is zero for the unordered phase and non-zero for the ordered phase [2]. As an example, consider a magnet: The magnetization is an order parameter, because it is zero for the unordered system with randomly oriented spins and non-zero for the ordered system with aligned spins. A local order parameter is one that can be defined for every point x in the material by considering only a small region around x. In the example of the magnet, the magnetization $M(x)$ at a point x can be determined by averaging the atomic magnetizations in a small region of space around x.

More recently, phases of matter have been found that cannot be described by a local order parameter [3]. That means that a phase transition between such a so-called topological phase and another phase cannot be described by considering only a small portion of the material: To define an order parameter for such a transition, the entirety of the material needs to be taken into account.

The use of non-local parameters to define distinct classes of phases is reminiscent of topology in mathematics. Topology studies classes of objects that can be deformed into each other smoothly, i.e. without tearing or gluing. One intuitive "order parameter" used in topology is the number of holes in a closed surface, called its genus. When a surface is smoothly deformed, this number does not change [4]. Therefore, the genus is called a topological invariant. This is an evidently non-local property: It is impossible to find the number of holes by just knowing a small part of a surface.

The non-local order parameters characterizing topological phases are called topological invariants, too. These are invariant under smooth, symmetry-respecting deformations of the physical system. This will be discussed in more detail in section 2.1. Topological phases can exhibit a number of unique experimentally observable properties. These include conducting edge states (a conducting state on the edge of an insulating material), the integer quantum Hall effect (a quantization of the Hall conductivity that depends only on natural constants), the fractional quantum Hall effect (a similar quantization of the Hall conductance based on quasi-particles with fractionalized elementary charge) and many more [3].

Recently, computational methods for identifying such topological phases based on tracking so-called Wannier charge centers have emerged (see section 2.3) [5]. These were further developed and implemented in the software package Z2Pack [1]. Specifically, Z2Pack provides an easy-to-use library for calculating two important topological invariants, the Chern number and the Z_2 invariant. Automatic convergence monitoring allows for high-throughput applications, such as the screening of materials databases for topologically interesting materials.

The topological classification of materials can be enriched by considering additional symmetries of a system. This allows for the splitting of the total Chern number into n individual Chern numbers, where n is the number of symmetry eigenspaces [6]. In this semester thesis, we develop numerical methods for identifying individual Chern numbers from so-called overlap matrices. These methods are integrated into Z2Pack and tested for the Haldane model.

This text is organized as follows: Section 2 presents an overview of the method used in Z2Pack to calculate topological invariants and introduces the idea of individual Chern numbers in more detail. In section 3, the necessary theory for calculating individual Chern numbers from overlap matrices is developed. Section 4 focuses on details of the implementation in Z2Pack and provides a guide for using the feature. In addition, a modified version of the Haldane model is presented as an example.

2 Background

In this section, we present some of the theory of topological invariants and their numerical calculation. We focus only on gapped Hamiltonians, i.e. Hamiltonians of systems whose band structure has an energy gap and the occupied states completely fill the band below the gap. It is possible to extend the theory to metals by restricting the calculations to a surface or line in the Brillouin zone (see ref. [1] for details).

2.1 Topological invariants

Topological invariants for physical systems are defined analogously to those in topology. Therefore, we need a physical analogue for the surfaces and smooth deformations used in topology.

The analogue of a surface in topology is the band structure of the material in physics. The analogue of a smooth deformation is an adiabatic change of the Hamiltonian that does not involve a direct gap closure, i.e. the valence and conduction band must not touch at any point in reciprocal space. An adiabatic change to the Hamiltonian can be thought of as a change that depends continuously on some parameters. This means the adiabatic change can, in principle, be performed infinitely slowly by varying its parameters infinitely slowly. In that case, it can be proven that the groundstate of the system follows the change of the Hamiltonian in the sense that the systems always stays in the groundstate of every intermediate Hamiltonian in the transition from initial to final Hamiltonian. This is called the adiabatic theorem [7, 8].

Therefore, we make the following definition: Two materials belong to the same topological class if and only if their Hamiltonians can be adiabatically transformed into each other without a direct gap closure and while respecting the symmetries of the system. Operationally, this means the following: One is given two systems with two gapped Hamiltonians H_0 and H_1. If one manages to find a continuous function $H(\lambda)$ such that (i) $H(0) = H_0$ and $H(1) = H_1$ and (ii) for all $\lambda \in [0, 1]$, $H(\lambda)$ is a Hamiltonian whose band structure does not have a direct gap closure, then the two Hamiltonians are in the same topological class. It important to point out that the existence of one such function $H(\lambda)$ suffices, i.e. not every adiabatic change connecting the two Hamiltonians must fulfill the gap-closure condition.

Topological invariants are quantities that can be calculated from the quantum-mechanical state of a system and that are constant within a topological class. They can therefore be thought of as an indexing system for topological classes: Any topological class is defined by the values the topological invariants take on it. This means that knowing of more topological invariants allows for a more fine-grained classification of topological classes. This is what motivates the decomposition of the Chern number C into individual Chern numbers C_i that was mentioned in section 1. Considering only the total Chern number, we might miss the division of, for example, the topological class with $C = 0$ into two different topological classes $C_1 = 0, C_2 = 0$ (topologically trivial) and $C_1 = -1, C_2 = 1$ (topologically interesting).

One immediate consequence of our definition of topological invariants is the existence of conducting edge states: If two materials with Hamiltonians H_1 and H_2 share a surface, the Hamiltonian must adiabatically change from H_1 to H_2 across the surface. If the materials belong to different topological classes, this means that there must be a direct gap closure, which implies electrical conduction.

2.2 Wannier functions

Typically, Bloch states, i.e. eigenstates of the Hamiltonian, are used as a basis set of the entire Hilbert space of states. The occupied states form a subspace of this Hilbert space. In the simple case of a gapped insulator, the occupied states are all states whose energy

eigenvalues lie below a fixed energy E_F, called the Fermi energy. We label the Bloch states by $|\psi_{n\bm{k}}\rangle$. By Bloch's theorem, the wavefunctions $\psi_{n\bm{k}}(\bm{r}) = \langle \bm{r}|\psi_{n\bm{k}}\rangle$ are modulated plane waves. In particular, they are very delocalized. We seek to construct states with more localized wavefunctions.

The most localized function possible is a δ-function. Formally, the δ-function can be written as an integral over equally weighted plane waves: $\delta(x) = \frac{1}{2\pi}\int e^{ikx}dk$. It is therefore reasonable to assume that integrating over all possible Bloch wavefunctions belonging to the same band n will also yield a localized wavefunction in the neighborhood of 0:

$$w_n(\bm{r}) \coloneqq \frac{V}{(2\pi)^3}\int_{\mathrm{BZ}} d\bm{k} \; \psi_{n\bm{k}}(\bm{r})\,.$$

The integral runs over the first Brillouin zone, because this is the set of all possible $\bm{k}$ for the Bloch states. V is the volume of the real space primitive unit cell. The factor in front of the integral is needed for normalization. It can be proven that $w_n(\bm{r})$ is indeed localized around 0 [9].

To find similar functions around other lattice points $\bm{R}$, we can simply translate $w_n(\bm{r})$ by $\bm{R}$. Writing $\psi_{n\bm{k}} = u_{n\bm{k}}(\bm{r})e^{i\bm{k}\bm{r}}$ with a lattice periodic function $u_{n\bm{k}}(\bm{r}) = u_{n\bm{k}}(\bm{r} + \bm{R})$, we can express the translated version of w_n as

$$
\begin{aligned}
w_n(\bm{r} - \bm{R}) &= \frac{V}{(2\pi)^3}\int_{\mathrm{BZ}} d\bm{k} \; \psi_{n\bm{k}}(\bm{r} - \bm{R}) \\
&= \frac{V}{(2\pi)^3}\int_{\mathrm{BZ}} d\bm{k} \; \psi_{n\bm{k}}(\bm{r})e^{-i\bm{k}\bm{R}}\,.
\end{aligned}
$$

This transformation is an inverse Fourier transform in $\bm{k}$. The resulting states are called Wannier states:

$$|\bm{R}n\rangle = \frac{V}{(2\pi)^3}\int_{\mathrm{BZ}} d\bm{k} \; |\psi_{n\bm{k}}\rangle \, e^{-i\bm{k}\bm{R}}\,. \tag{2.1}$$

These form a basis of the Hilbert space.

Notice that $|\bm{R}n\rangle$ as defined here is a superposition of Bloch states in the n-th band, i.e. no mixing of bands occurs. If n_F is the index of the (completely filled) valence band, then the Wannier states $\{|\bm{R}n\rangle \mid n \leq n_F, \bm{R} \text{ lattice vector}\}$ form a basis of the subspace of occupied states.

The construction of Wannier states is not unique, because the Bloch states can be multiplied by an arbitrary, $\bm{k}$-dependent phase $e^{i\phi(\bm{k})}$. This is often called gauge freedom. A priori, there is no preferred choice of phase. One numerically convenient criterion for choosing a phase is to require that the Wannier states have minimal spread in position, i.e. that they are maximally localized around the lattice point $\bm{R}$ [10]. The Wannier functions one obtains with this choice of gauge (phase) are called maximally localized Wannier function (MLWFs). In the maximal localization procedure, Bloch states of different bands within the occupied subspace can be mixed, but no mixing occurs between the occupied and unoccupied bands. As a result, the MLWFs still form a basis of the occupied states. For a more detailed introduction, see ref. [11].

We can also apply the inverse Fourier transform not along all axes in reciprocal space, but just along the k_x-axis:

$$|R_x, k_y, k_z; n\rangle = \frac{V}{(2\pi)^3}\int_{\mathrm{BZ}} dk_x \, |\psi_{n\bm{k}}\rangle \, e^{-ik_x R_x}\,. \tag{2.2}$$

If we apply the maximal localization criterion along this axis, we will end up with so-called maximally localized hybrid Wannier functions (MLHWFs).

2.3 Wannier charge centers

For every energy band n, the Wannier charge center (WCC) of that band is defined as the position expectation value of the Wannier function around 0:

$$\overline{x}_n = \langle \mathbf{0}, n | \, \hat{\mathbf{r}} \, | \mathbf{0}, n \rangle \, .$$

For the following, WCCs of hybrid Wannier functions will be more useful:

$$\overline{x}_n(k_y, k_z) = \langle 0, k_y, k_z; n | \, \hat{r}_x \, | 0, k_y, k_z; n \rangle \, .$$

Like the Wannier functions, the WCCs are gauge-dependent. However, the physically relevant quantity we will be interested in is the sum of all WCCs across the occupied bands $P = \sum_{n \leq n_F} \overline{x}_n$, and this sum turns out to be gauge-invariant. It has a physical interpretation relating to the polarization of a dielectric [12].

2.4 Berry's phase for Bloch functions

For the numerical calculation of WCCs, it is useful to write them in terms of the so-called Berry's phase [13]. Here, we give a short introduction to Berry's phase and its generalization to Bloch functions.

Consider a system with a Hamiltonian that can adiabatically change with some parameter λ. We periodically vary λ with time, $\lambda(t + T) = \lambda(t)$, and perform this change slowly enough so that the system always stays in the same energy eigenstate $|n(\lambda)\rangle$ (by the adiabatic theorem). From basic quantum mechanics, we know that the state will pick up a phase factor

$$\gamma_{E,n}(t) = \int_0^t \frac{-E_n(\lambda(t'))}{\hbar} dt' \, .$$

In addition, the state can also pick up a geometrical phase factor, i.e. one which depends on the geometry of the parameter space in which λ is varied. This phase is called Berry's phase $\gamma_{B,n}(t)$. Therefore, the time-evolution of $|n(\lambda = 0)\rangle$ with an adiabatically changing Hamiltonian is

$$|\psi(t)\rangle = \underbrace{\exp(i\gamma_{E,n}(t))}_{\substack{\text{Phase from time} \\ \text{evolution operator}}} \underbrace{\exp(i\gamma_{B,n}(t))}_{\text{Berry's phase}} \underbrace{|n(\lambda(t))\rangle}_{\substack{\text{Adiabatically changed} \\ \text{energy eigenstate of} \\ \text{Hamiltonian } H(\lambda(t))}} \, .$$

Inserting this ansatz into the time-dependent Schrödinger equation $H(\lambda(t)) |\psi(t)\rangle = i\hbar |\psi(t)\rangle$, one finds

$$\frac{d}{dt}\gamma_B(\lambda(t)) = i \langle n(\lambda(t)) | \, \partial_\lambda \, |n(\lambda(t))\rangle \frac{d}{dt}\lambda(t) \, .$$

Integrating this expression over time and changing the integration variable to λ yields

$$\gamma_{B,n}(C) = \int_C i \langle n(\lambda) | \, \partial_\lambda \, |n(\lambda)\rangle \, d\lambda \, , \tag{2.3}$$

where C is the curve along which λ changes in parameter space. Significantly, Berry's phase can be non-zero even if C is a closed loop, i.e. the initial and final Hamiltonian are the same. In that case, $\gamma_B(C)$ depends only on the geometry of the loop in parameter space. For this reason, Berry's phase is often called a geometric phase.

For crystalline solids, the Bloch functions depend smoothly on $\mathbf{k}$ for $\mathbf{k}$ inside the first Brillouin zone. This allows us to define Berry's phase, with $\mathbf{k}$ playing the role of the parameter λ [14]:

$$\gamma_{B,n}(C) = \int_C i \langle u_{n\mathbf{k}} | \, \partial_{\mathbf{k}} \, |u_{n\mathbf{k}}\rangle \, d\mathbf{k} \, , \tag{2.4}$$

with $\partial_{\boldsymbol{k}} = (\partial_{k_x}, \partial_{k_y}, \partial_{k_z})$ and C a curve inside the Brillouin zone. For this definition, an adiabatically changing Hamiltonian $H(\lambda(t))$ is no longer necessary, because Bloch's theorem provides a smoothly varying parameter $\boldsymbol{k}$ for the energy eigenstates of a constant Hamiltonian H.

2.5 Wannier charge centers from Berry's phase and overlap matrices

Our goal in this section is to find an expression for the Wannier charge centers in terms of Berry's phase. For simplicity of notation, we restrict ourselves to a 1-dimensional crystal with lattice constant a and a single band. As a first step, we write the Bloch function $\psi_{n,k}(x)$ in terms of the Wannier functions $w_{n,ma}$ by applying a Fourier transform to (2.1), dropping the index n for readability:

$$\psi_k(x) = \frac{1}{\sqrt{N}} \sum_m e^{ikma} w_{ma}(x)\,.$$

The integral is replaced by a sum because the real space lattice vectors are discrete. N is the number of unit cells in the crystal. The factor $1/\sqrt{N}$ is needed for normalization.

Using $\psi_k(x) = u_k(x) e^{ikx}$:

$$u_k(x) = \frac{1}{\sqrt{N}} \sum_m e^{ik(ma-x)} w_{ma}(x)\,. \tag{2.5}$$

We can insert this expression into (2.4) with C being the line across the entire 1-dimensional Brillouin zone:

$$
\begin{aligned}
\gamma_B &= \int_{-\pi/a}^{\pi/a} dk \; i \, \langle u_{nk} | \, \partial_k \, | u_k \rangle \\
&= \sum_{l,m} \frac{1}{N} \int_{-\pi/a}^{\pi/a} dk \; i \int_{\mathbb{R}} dx \; w_{la}^*(x) \, i(ma - x) \, w_{ma}(x) \\
&= \frac{2\pi}{a} \frac{1}{N} \sum_m \int_{\mathbb{R}} dx \; w_0^*(x - ma) \, (x - ma) \, w_0(x - ma) \\
&= \frac{2\pi}{a} \int_{\mathbb{R}} dx \; w_0^*(x) \; x \; w_0(x) \\
&= \frac{2\pi}{a} \overline{x}\,,
\end{aligned}
$$

where we made use of the orthogonality of Wannier functions and their translation property in the third equality.

To numerically calculate Berry's phase, we need to discretize the integral and derivative to values k_i with step size Δk:

$$
\begin{aligned}
\gamma_B &= i \sum_i \Delta k \, \langle u_{k_i} | \frac{u_{k_{i+1}} - u_{k_i}}{\Delta k} \rangle \\
&= i \sum_i \langle u_{k_i} | u_{k_{i+1}} \rangle - 1\,. \tag{2.6}
\end{aligned}
$$

The state $|u_k\rangle$ is rotated in Hilbert space as k changes. For sufficiently small discretization, the overlap $\langle u_{k_i} | u_{k_{i+1}} \rangle$ gives the angle by which the state is rotated in the step $i \to i+1$. Thus, we may write $\langle u_{k_i} | u_{k_{i+1}} \rangle = e^{i\phi_i}$, where ϕ_i is a small angle. Taylor-expanding the exponential to first order in ϕ_i and inserting the expansion into (2.6) gives

$$\gamma_B = -\sum_i \phi_i\,.$$

We see that Berry's phase is just the total angle by which the state was rotated in Hilbert space. We can rewrite this as a product of overlaps:

$$\gamma_B = -\arg\left(\prod_i \langle u_{k_i}|u_{k_{i+1}}\rangle\right). \tag{2.7}$$

We have therefore found an expression for the WCCs $\overline{x} = \frac{a}{2\pi}\gamma_B$ in terms of the overlaps of adjacent Bloch functions.

The generalization of this method for multi-band systems uses unitary rotation matrices instead of angles and overlap matrices instead of single overlaps to describe the rotation of all the states $|u_{nk}\rangle$ as k changes. The overlap matrix of two adjacent k-points in a system with n_0 filled bands is defined as

$$M_{lm}^{k_i \to k_{i+1}} = \langle u_{lk_i}|u_{mk_{i+1}}\rangle, \quad l,m \in \{1,\ldots,n_0\}.$$

Multiplying the overlap matrices together yields the so-called Wilson loop:

$$W = \prod_i M^{k_i \to k_{i+1}}.$$

The eigenvalues λ_n of the Wilson loop are closely related to the WCCs:

$$\overline{x}_n = -\frac{a}{2\pi}\arg\lambda_n. \tag{2.8}$$

Notice the similarity of this expression with (2.7): The role of individual overlaps is taken by the overlap matrices and to extract rotation angles from the Wilson loop, we need to find its eigenvalues. We do not prove (2.8) here. A more detailed exposition can be found in refs. [1, 15].

2.6   Chern number from Wannier charge centers

The reason we are interested in Wannier charge centers is that they are closely related to two important topological invariants, the Chern number and the Z_2-invariant. In this section, we describe the scheme used by Z2Pack to calculate these topological invariants [1]. We consider a two-dimensional crystal with lattice constant $a = 1$ for simplicity. For other lattice constants, normalization factors are needed.

The Brillouin zone of such a system is a square with side-length 2π, with sides parallel to k_x and k_y, respectively. We discretize the k_y axis, so the Brillouin zone may be thought of as a number of lines in the k_x- direction placed next to each other. Each of these lines can now be treated as a 1-dimensional system as in section 2.5. In particular, we can calculate the Wilson loop along each of the lines and obtain the Wannier charge centers by finding the eigenvalues. The sum of the charge centers is called the polarization $P = \sum \overline{x}_n$.

The calculation of the polarization can be repeated for all other lines, each parameterized by a fixed k_y. Therefore, the polarizations for all of the lines define a function $P(k_y)$.

The Chern number is then given by

$$C = P(k_y = 2\pi) - P(k_y = 0). \tag{2.9}$$

This number corresponds to the Chern number known from topology in mathematics. The proof of this formula makes use of Berry's phase and can be found in ref. [16, section 4.3].

The techniques presented so far allow us to numerically calculate the Chern number of any Hamiltonian in 2 dimensions and are implemented in Z2Pack [1].

This method is generalized for three dimensional systems by choosing a plane in the Brillouin zone. This plane can be treated in the same way as the 2-dimensional Brillouin zone of a 2-dimensional system. In Z2Pack, this plane is provided as an input by the user.

2.7 Topological invariants in symmetry eigenspaces

We now consider a Hamiltonian H with an additional unitary symmetry S, i.e. $S^\dagger S = \mathbb{1}$ and $[H, S] = 0$. The symmetry splits the Hilbert space into a sum of symmetry eigenspaces

$$\mathcal{H} = \bigoplus_\lambda \text{Eig}_\lambda(S),$$

each of which is an invariant subspace of the Hamiltonian. (This follows from commutation: $v \in \text{Eig}_\lambda(S) \Rightarrow SHv = HSv = \lambda Hv \Rightarrow Hv \in \text{Eig}_\lambda(S)$.) We can therefore restrict the Hamiltonian to any of the symmetry eigenspaces:

$$H_\lambda := H\big|_{\text{Eig}_\lambda(S)}.$$

Each of the H_λ can be treated just like any other Hamiltonian and we can define and calculate its topological invariants just like before. For this to be of any use, the individual topological invariants must still be invariant under adiabatic transformations that do not cause a direct gap closure. This is indeed the case as long as the adiabatic transformation respects the symmetry, i.e. for all intermediate Hamiltonians $H(\tau)$ in the transformation, $[H(\tau), S] = 0$.

To prove this, assume the existence of some adiabatic transformation $H(\tau)$ without a direct gap closure and $[H(\tau), S] = 0 \,\forall \tau$ that changes the individual topological invariant on $\text{Eig}_\lambda(S)$. That implies a direct gap closure of the energy bands of H_λ, i.e. two states $|\alpha_\lambda(\tau)\rangle, |\beta_\lambda(\tau)\rangle \in \text{Eig}_\lambda(S) \subset \mathcal{H}$ with the same energy eigenvalue for some τ'. Because $\text{Eig}_\lambda(S)$ is invariant under $H(\tau')$, acting with the complete Hamiltonian $H(\tau')$ on $|\alpha_\lambda(\tau')\rangle, |\beta_\lambda(\tau')\rangle$ gives the same result as acting with $H_\lambda(\tau')$ on $|\alpha_\lambda(\tau')\rangle, |\beta_\lambda(\tau')\rangle$. Therefore, H must also have a direct gap closure, which contradicts the assumption.

Phases with non-zero individual Chern numbers are only topologically non-trivial as long as the symmetry is respected. This is why they are called symmetry-protected topological phases [1].

If such a splitting is done for the Chern number, it can be proven [1, appendix E] that the total Chern number is the sum of the individual ones:

$$C = \sum_\lambda C_\lambda. \tag{2.10}$$

2.7.1 Z_2-Invariant

The Z_2-invariant can be understood in the context of individual Chern numbers for time-reversal symmetry.

For a Hamiltonian H that is invariant under (anti-unitary) time-reversal Θ, i.e. $[H, \Theta] = 0$, spin-1/2 particles like electrons particles form so-called Kramer pairs. A Kramer pair is a pair of states that are mapped to each other under time-reversal, and because spin-1/2 particles are not invariant under time reversal, the two states forming a Kramer pair are distinct [17]. The Hilbert space can be split into two subspaces such that every Kramer pair is made up of one state in each subspace. This splitting is not unique because the assignment of the first state of every Kramer pair to a subspace is arbitrary. Let one such splitting be $\mathcal{H} = \mathcal{H}_1 \oplus \mathcal{H}_2$.

Th Chern number is odd under time-reversal, because time-reversal changes the direction of the k_y-axis while leaving the polarization invariant. The reversal of the k_y-direction causes the Chern number to pick up a minus sign. Therefore, a time-reversal invariant system must have Chern number 0. Because the total Chern number is given by the sum of the individual ones, the two individual Chern numbers C_1, C_2 must be equal in magnitude and opposite in sign.

The individual Chern numbers C_1, C_2 in the Hilbert subspaces $\mathcal{H}_1, \mathcal{H}_2$ can be non-zero and their difference $C_1 - C_2$ must be an even number. When the Hamiltonian is adiabatically changed while preserving time-reversal invariance or the assignment of states in a Kramer pair to $\mathcal{H}_1$ and $\mathcal{H}_2$ is reversed, it can be shown that the individual Chern numbers can only change by an even number [18]. Therefore, the difference $C_1 - C_2$ can only change by multiples of 4, so the parity of $(C_1 - C_2)/2$ is preserved. This defines the Z_2-invariant for time-reversal symmetric systems:

$$Z_2 = \frac{C_1 - C_2}{2} \mod 2\,.$$

In practice, one does not need to calculate the individual Chern numbers. Instead, the Z_2-invariant can be calculated from the number of crossings of the polarization with an arbitrary line from $k_y = 0$ to $k_y = \pi/a_y$, where a_y is the lattice constant in the y-direction. Refs. [5, 1] provide more detail on this.

3   Projection of overlap matrices

As outlined in section 2, the calculation of WCCs is based on overlap matrices. To find the Chern number in a symmetry eigenspace as described in section 2.7, we need to find a way to project those overlap matrices onto the symmetry eigenspace. In this section, we solve this problem in full generality for two arbitrary Hamiltonians, each with a symmetry. The only constraint on the symmetries is that they need to have the same spectrum.

First, we establish the notation and formulate the problem using this notation in section 3.1. Then, we solve the projection problem for systems with explicit Hamiltonians (section 3.2) and for the output of first principles calculations (section 3.3). Theorems 3.1 and 3.2 summarize the main results. Finally, in section 3.4 the methods for projecting overlap matrices are applied to the Wilson loop used for calculating WCCs.

3.1   Notation

Consider two Hamiltonians $\tilde{H}^1, \tilde{H}^2$ and two unitary symmetries $\tilde{S}^1, \tilde{S}^2$ operating on an n-dimensional Hilbert space $\tilde{\mathcal{H}}$, s.t. $[\tilde{H}^i, \tilde{S}^i] = 0$. Furthermore, we assume both symmetries to have the same eigenvalues with the same degeneracies. Because the $\tilde{H}^i$ are hermitian, they have a complete set of orthonormal eigenstates, denoted $\{\tilde{u}^i_j\}$, where $i \in \{1, 2\}$ and $j \in \{1, \ldots, n\}$. Of these n eigenstates, only the first l are occupied, meaning that only the first l eigenstates have eigenvalues smaller than some constant E_F. These span the Hilbert spaces of occupied states $\mathcal{H}^i$ with the basis $\{u^i_j\}$.

The occupied space $\mathcal{H}^i$ is invariant under the action of $\tilde{S}^i$, since for any $u^i \in \mathcal{H}^i : \tilde{H}^i \tilde{S}^i u^i = \tilde{S}^i \tilde{H}^i u^i = \lambda \tilde{S}^i u^i$, where the eigenvalue λ is smaller than E_f. Thus, $Su^i \in \mathcal{H}^i$. The restrictions of $\tilde{H}^i$ and $\tilde{S}^i$ to the space of occupied states are denoted by H^i and S^i.

In summary, all objects concerning the whole Hilbert space (dimension n) are written with a tilde. All objects concerning the subspace of occupied states (dimension l) are written without a tilde.

Our goal is to find the overlap matrix M^λ of the occupied eigenstates projected onto a selected symmetry eigenspace with eigenvalue λ. To do so, we choose bases $\{\xi^i_j\}_{1 \le j \le m}$ of $\mathcal{H}^i \cap \mathrm{Eig}_\lambda(S^i)$ for each Hamiltonian, where we assume $\dim \mathcal{H}^1 \cap \mathrm{Eig}_\lambda(S^1) = \dim \mathcal{H}^2 \cap \mathrm{Eig}_\lambda(S^2) =: m$. We do this for some fixed λ, so we can omit the index λ for the ξ^i_j.

Given these bases, M^λ is given by

$$M^\lambda = \begin{pmatrix} \langle \xi_1^1 | \xi_1^2 \rangle & \cdots & \langle \xi_1^1 | \xi_m^2 \rangle \\ \vdots & & \vdots \\ \langle \xi_m^1 | \xi_1^2 \rangle & \cdots & \langle \xi_m^1 | \xi_m^2 \rangle \end{pmatrix} . \tag{3.1}$$

Therefore, the problem reduces to finding the bases $\{\xi_j^i\}$ given the available information in each case.

3.2 Systems with an explicit Hamiltonian

For systems with a known hamiltionian, we can calculate the eigenbasis $\{u_j^i\}$ of the occupied subspace explicitely. The symmetry matrix $\tilde{S}^i$ is given in the standard basis of $\tilde{\mathcal{H}}$. Notice that we do not have access to the restricted symmetry matrix S^i in this case.

For a fixed i and symmetry eigenvalue λ (both of which we suppress for readibility), let $U \in \mathbb{C}^{n \times l}$ be the column matrix of $\{u_j\}$ and $\tilde{V} \in \mathbb{C}^{n \times m}$ the column matrix of the orthonormal basis of $\mathrm{Eig}_\lambda(\tilde{S})$, where $m = \dim(\mathrm{Eig}_\lambda(\tilde{S}))$.

The projection of u_j onto $\mathrm{Eig}_\lambda(\tilde{S})$ is given by

$$P_\lambda(u_j) = V V^\dagger u_j .$$

In general, the projected eigenvectors are linearly dependent, as $\dim(\mathcal{H} \cap \mathrm{Eig}_\lambda(\tilde{S})) \leq \dim(\mathcal{H})$. If we select a linearly independent subset, we can use these as the basis $\{\xi_j\}$.

Numerically, the most efficient method for this is to LU-decompose the matrix $P_\lambda(U)$, defined as the column matrix of $P_\lambda(u_j)$, and only keep the upper triangular matrix. We denote this operation by $\mathcal{LU}$.

Therefore, we can write

$$X = \mathcal{LU}(V V^\dagger U) \overset{!}{=} U A ,$$

where X is the column matrix of $\{\xi_j\}$ and $A = (A_{kj})$ are the coefficients of the linear expansion of the basis vectors of $\mathcal{H} \cap \mathrm{Eig}_\lambda(\tilde{S})$ in the original occupied eigenbasis $\{u_j\}$. We have found an expression for the coefficients A_{kj} in terms of quantities we know:

$$A = U^\dagger \mathcal{LU}(V V^\dagger U) . \tag{3.2}$$

Reintroducing the superscripts to distinguish between the Hamiltonians and plugging this result into equation (3.1) yields the desired expression for M^λ:

$$\begin{aligned} M_{ij}^\lambda &= \langle \xi_i^1 | \xi_j^2 \rangle \\ &= \sum_{p,q} A^{1*}_{pi} A^2_{qj} \langle u_p^1 | u_q^2 \rangle \\ &= \sum_{p,q} A^{1*}_{pi} A^2_{qj} M_{pq} . \end{aligned}$$

Theorem 3.1 *Let $A^i = U^{i\dagger} \mathcal{LU}(V V^\dagger U^i)$, where V is the column matrix of an orthonormal basis of $\mathrm{Eig}_\lambda(\tilde{S})$ and U^i is the column matrix of an orthormal basis of the occupied subspace $\mathcal{H}^i$. Then, the projected overlap matrix M^λ is given by*

$$M^\lambda = A^{1\dagger} M A^2 . \tag{3.3}$$

3.3   First-principles systems

For first-principles systems, the symmetries are represented in the occupied eigenbasis $\{u_j^i\}$ of the respective Hamiltonian:

$$D^i = \begin{pmatrix} \langle u_1^i | S^i | u_1^i \rangle & \cdots & \langle u_1^i | S^i | u_l^i \rangle \\ \vdots & & \vdots \\ \langle u_l^i | S^i | u_1^i \rangle & \cdots & \langle u_l^i | S^i | u_l^i \rangle \end{pmatrix} . \tag{3.4}$$

We want to find an expression for ξ_j^i only in terms of the unprojected overlap matrix $(M_{ij}) = (\langle u_i^1 | u_j^2 \rangle)$ and the symmetry matrices D^1 and D^2. In this case, we will additionally require that the bases $\{\xi_j^i\}$ are orthonormal for both i.

We express ξ_j as a linear combination of the occupied eigenbasis $\{u_k\}$ (the superscript indicating which Hamiltonian we are dealing with is suppressed for readibility):

$$\xi_j = \sum_k A_{kj} u_k .$$

Such an expansion always exists because $\xi_j \in \mathrm{Eig}_\lambda(S) \cap \mathcal{H}$ and $\{u_k\}$ forms a basis of $\mathcal{H}$. We find

$$\begin{aligned} \lambda \delta_{ij} &= \langle \xi_i | S | \xi_j \rangle \tag{3.5} \\ &= \sum_{p,q} A_{pi}^* A_{qj} \langle u_p | S | u_q \rangle \\ &= \sum_{p,q} A_{pi}^* A_{qj} D_{pq} . \end{aligned}$$

Written as a matrix equation with $A = (A_{ij})$:

$$A^\dagger D A = \mathrm{diag}(\lambda, ..., \lambda) . \tag{3.6}$$

Any A that satifsies (3.6) will produce ξ_i that satisfy (3.5). In particular, if we choose A to be the column matrix of an orthonormal eigenbasis of $\mathrm{Eig}_\lambda(D)$, (3.6) is satisfied. Using the same calculation as in section 3.2, we find:

Theorem 3.2 *Let A^i be the column matrix of an orthonormal eigenbasis of $\mathrm{Eig}_\lambda(D^i)$. The projected overlap matrix M^λ is given by*

$$M^\lambda = A^{1\dagger} M A^2 . \tag{3.7}$$

3.4   Projection of the Wilson loop

So far, we have considered the general case of two independent Hamiltonians. To formulate the projection formula for the Wilson loop, we return to a k-dependent Hamiltonian $H(k_i)$, where the k_i form a line in reciprocal space. Let A^{k_i} be the matrix A as defined in theorems 3.1 or 3.3 belonging to the Hamiltonian $H(k_i)$. Then, the Wilson loop along the k_i can be projected onto $\mathrm{Eig}_\lambda(S)$ as follows:

$$W^\lambda = \prod_i A^{k_i \, \dagger} M^{k_i \to k_{i+1}} A^{k_{i+1}} . \tag{3.8}$$

4   Implementation and usage

In this section we give a short overview of the format in which the symmetry data is given, explain how the projection of overlap matrices presented in the previous section is implemented in Z2Pack and give a guide to using this feature. Finally, a modified Haldane model is presented as an example.

4.1 Format of symmetry data

As shown in section 3, different representations of a symmetry are needed depending on whether the eigenstates of the Hamiltonian or just its overlap matrices are known.

For systems with an explicit Hamiltonian, the symmetry is given by the user as a matrix. This matrix is the representation matrix of the symmetry map in the basis of the Hilbert space that is also used for the Hamiltonian matrix.

For first-principles systems calculated using the QuantumEspresso package [19, 20], the symmetry matrix is given in the basis of the occupied states of the Hilbert space. The calculation of the symmetry matrix in this basis is presented in ref. [21]. Specifically, eq. (17) of ref. [21] defines the matrix $\tilde{d}_{mn}$ as the representation matrix of the symmetry in the basis of the occupied Kohn-Sham orbitals. The code `pw2wannier90.f90` from the QuantumEspresso package calculates these matrices and writes them in a file `seedname.dmn`, where `seedname` is a user-provided variable. The specification of the `.dmn`-format can be found in [22, section 5.4]. Z2Pack reads the `seedname.dmn` file, selects the symmetries that leave every point on the specified surface invariant and writes these symmetries to a `seedname.sym` file to be used by `pw2wannier90.f90`. The specification of the `.sym` format is given in [22, section 5.6.2].

4.2 Implementation in Z2Pack

The existing architecture of Z2Pack divides the calculation of topological invariants into three distinct steps [1]:

First, a `System` object is created. This object contains all the relevant information about the system at hand: For systems with an explicit Hamiltonian, the Hamiltonian itself specifies a `System`. For first-principles systems, the input files and parameters needed for the first-principles calculation constitute the `System`. In both cases, a number of optional parameters can be passed to the system if desired.

Next, a surface run is performed. This means that for a user-specified surface in the Brillouin zone, a set of lines is created and the overlap matrices for points along those lines are calculated as described in section 2.6. In Z2Pack, each of the lines is represented as an `OverlapLineData` object. All of the `OverlapLineData` objects are bundled into a `SurfaceData` object. Performing a surface run returns a `SurfaceResult` object, which contains the `SurfaceData` object as well as convergence information.

Finally, the Chern number and Z_2-invariant of the surface can be calculated. This is done by passing a `SurfaceResult` object to the `z2pack.invariant.chern` or `z2pack.invariant.z2` functions. The calculation of WCCs does not happen until an invariant is calculated.

The guiding principle in implementing the calculation of symmetry-restricted topological invariants was to maintain full backwards-compatibility and to require minimal changes to existing calculations when updating them to include symmetries.

The symmetry of the system is stored in the `System` object as an explicit symmetry matrix in the case of systems with an explicit Hamiltonian or as a path to the `seedname.dmn` file in the case of Quantum Espresso calculations. During the surface run, symmetry matrices are saved for each k-point of a line in the `OverlapLineData` object. The surface run with symmetries returns a `SurfaceResult` object that can be used in exactly the same way as the result of a run without symmetries.

To make use of the symmetries stored in the `OverlapLineData` objects, the surface result is projected onto a symmetry eigenspace. Specifically, a new `SurfaceData` object is created with the same set of lines as the original one, but with all overlap matrices projected onto a symmetry eigenspace as described in section 3. The projected surface does not store the

symmetries or convergence information of the original surface to conserve memory.

The projection of a surface does not modify the original surface, but instead creates a new one. Therefore, all convergence and symmetry information can still be accessed through the original `SurfaceResult` object. The projected surface can be used like any other surface to calculate topological invariants.

4.3 Usage

4.3.1 Systems with an explicit Hamiltonian

For systems with explicit Hamiltonians, the symmetry must be specified as a matrix in the same basis as the Hamiltonian, that is the symmetry matrix S must be a matrix that commutes with the Hamiltonian matrix $H(k)$ for every k. The symmetry matrix is passed to the system via the `symm` keyword argument.

The surface run needs to be performed with `use_symm = true`. We will call the return value of this command `surface_result` in the following. To project the surface result, the command `surface_result.symm_project(symmetry_eigenvalue)` is used, where `symmetry_eigenvalue` is the eigenvalue of the symmetry eigenspace onto which the surface is projected. The projected surface result can be used like any other surface result, except that it does not contain convergence information.

4.3.2 First-principles systems

The implementation in Z2Pack works for first-principles systems calculated using QuantumEspresso [19, 20]. Currently, only systems without spin-orbit coupling and without non-colinear magnetism can be used. This is due to a limitation in `pw2wannier90.f90`, a part of the Quantum Espresso package, that restricts the calculation of the $\tilde{d}_{mn}$-matrices to these cases.

To use symmetry projection for first-principles systems, the following input parameters need to be set in the input files of the first-principles calculation:

- In `seedname.scf.in` (input for self-consistent calculation): `noncolin = .false.` and `lspinorb = .false.`

- In `seedname.nscf.in` (input for non-self-consistent calculation): `noncolin = .false.` and `lspinorb = .false.`

- In `seedname.pw2wan.in` (input for `pw2wannier90.f90`): `read_sym = .true.` and `write_dmn = .true.`

- In `seedname.win` (input for Wannier90): The projections used by Wannier90 need to be manually given so that the space spanned by the projection orbitals is invariant under the particular symmetry under consideration. For example, for a symmetry that swaps the x- and y-components and leaves the z-component invariant, the orbitals s, p_x, p_y work for this purpose, but the orbitals s, p_x, p_z do not, because p_x is mapped to p_y outside the subspace. If an unsuitable set of orbitals is chosen, the $\tilde{d}_{mn}$ matrices will not be unitary and Z2Pack will raise an error.

The first two settings are required due to the limitation in QuantumEspresso mentioned above and may not be needed in the future when QuantumEspresso is updated accordingly. The third setting is needed so `pw2wannier90.f90` only uses the local symmetries of the surface and outputs the $\tilde{d}_{mn}$ matrix used for projection onto a symmetry eigenspace.

Before the surface run is executed, the necessary symmetry input file for a specific surface needs to be generated. For QuantumEspresso, the function `gen_qe_symm_files` is provided

to do generate the `.sym` file used by `pw2wannier90.f90`. For other first-principles codes, a different function written by the user can be used. The `.sym` file needs to be included in the list of input files when the `System` is created in Z2Pack.

The surface run needs to be performed with the keyword argument `use_symm = true`. Because the first principles calculation will in general identify multiple symmetries, it is necessary to specify which symmetry should be used for projection. The index of the different symmetries is the same as in the `.sym` input file for QuantumEspresso. To project the surface result, the command `surface_result.symm_project(symmetry_eigenvalue, isym=symmetry_index)` is used, where `symmetry_index` is the index of the desired symmetry.

4.4 Example: Haldane model

The Haldane model [23] is a simple model of the quantum Hall effect without an external magnetic field to create Landau levels. This is achieved by considering a 2-dimensional honeycomb lattice with two sublattices so that nearest neighbors always belong to different sublattices. Introducing second-neighbor interactions, i.e. interactions between nearest neighbors in a sublattice, can break time-reversal invariance. This gives rise to quantum Hall behavior.

The Hamiltonian of the Haldane model can be represented in the basis $\{(\psi_A(\boldsymbol{k}), \psi_B(\boldsymbol{k})\}$, where $\psi_i(\boldsymbol{k})$ is the Bloch function with wave vector $\boldsymbol{k}$ on sublattice i:

$$H(\boldsymbol{k}, \phi) = 2t_2 \cos(\phi) c_B(\boldsymbol{k}) \mathbb{1} + t_1 c_A(\boldsymbol{k}) \sigma_1 + t_1 s_A(\boldsymbol{k}) \sigma_2 + (M - 2t_2 \sin(\phi) s_B(\boldsymbol{k})) \sigma_3 \,, \quad (4.1)$$

where $c_i(\boldsymbol{k}), s_i(\boldsymbol{k})$ are functions whose exact form is irrelevant for our purpose, t_i, M are parameters of the model and σ_i are the Pauli matrices. The Chern number of the Haldane model is odd in ϕ: The Chern number of $H(\boldsymbol{k}, s\phi)$ is $-s$ for $s \in \{+1, -1\}$.

We can form a block-diagonal Hamiltonian of multiple Haldane Hamiltonians

$$H_n(\boldsymbol{k}, \phi) = \underbrace{\begin{pmatrix} H(\boldsymbol{k}, \pm\phi) & & 0 \\ & \ddots & \\ 0 & & H(\boldsymbol{k}, \pm\phi) \end{pmatrix}}_{n \; 2 \times 2 \; \text{blocks}},$$

where the sign of ϕ can be chosen independently in each block. This Hamiltonian has the following symmetry:

$$S = \begin{pmatrix} 1 \cdot \mathbb{1}_2 & & 0 \\ & \ddots & \\ 0 & & n \cdot \mathbb{1}_2 \end{pmatrix} \,.$$

S is indeed a symmetry because each block of H commutes with the corresponding diagonal block of S. The spectrum of S is $\sigma_S = \{1, \ldots, n\}$.

We can calculate the i-th individual Chern number of H_n by projecting the Hamiltonian onto $\text{Eig}_i(S)$ for $i \in \{1, \ldots, n\}$. From the addition property of individual Chern numbers as in equation (2.10), we know that the Chern number of H_n is given by $C_n = n_- - n_+$, where $n_\pm$ are the number of blocks with $\pm\phi$.

We now present the code that performs these calculations with Z2Pack. First, we create functions to generate the block-diagonal Haldane Hamiltonian and its symmetry:

```
import scipy.linalg as la
import numpy as np
def Hamilton(k, m, t1, t2, phi, signs):
    return la.block_diag(*[Hamilton_Haldane(k, m, t1, t2, s * phi) for s in signs])
```

15

	Total Hamiltonian	Projection on $\text{Eig}_1(S)$	Projection on $\text{Eig}_2(S)$	Projection on $\text{Eig}_3(S)$
Sign of ϕ		+	-	-
Chern number	1	-1	1	1

Table 1: Chern numbers of total and projected Hamiltonians of block-diagonal Haldane model. As expected from theory, the Chern number on each projected Hamiltonian depends on the sign of ϕ. The total Chern number is given by the sum of the individual Chern numbers.

```python
def symmetry(n):
    return la.block_diag(*[np.diag([i, i]) for i in range(1, n + 1)])
```

`Hamilton_Haldane` is a function that returns the standard 2×2 Haldane Hamiltonian.

Next, we need to create a `System` object with this Hamiltonian and symmetry and perform a surface run with this system and the `use_symm` keyword argument set to `true`. Here, we use a Hamiltonian with three blocks, the first one with $+\phi$ and the other two with $-\phi$:

```python
m, t1, t2, phi = 0.5, 1., 1. / 3., 0.5 * np.pi # set parameters for Hamiltonian
signs = [1, -1, -1] # signs for phi
n = len(signs)
system = z2pack.hm.System(lambda k: Hamilton(k, m, t1, t2, phi, signs), symm=symmetry(n))

result = z2pack.surface.run(
    system=system,
    surface=lambda s, t: [t, s, 0.],
    use_symm=True
)
```

Finally, we can project the surface onto the different eigenspaces of the symmetry, remembering that the symmetry eigenvalues are $\sigma_S = \{1, \ldots, n\}$. For each projected surface, the Chern number can be calculated:

```python
projected_results = [result.symm_project(i) for i in range(1, n + 1)]
total_chern = z2pack.invariant.chern(result)
individual_chern = [z2pack.invariant.chern(r) for r in projected_results]
```

The results are as we expected and can be found in Table 1 and Figure 4.1.

5 Conclusion and outlook

We have introduced a numerical technique for projecting overlap matrices of a Hamiltonian onto symmetry eigenspaces. This method can be used in conjunction with the tracking of Wannier charge centers to calculate symmetry-protected topological invariants, such as individual Chern numbers. This method has been implemented as an extension of the software package Z2Pack [1]. We have demonstrated this technique for a modified version of the Haldane model. In addition, the calculation of individual Chern numbers of first-principles systems calculated using the QuantumEspresso package [19, 20] is possible, but limited to systems without spin-orbit coupling or non-colinear magnetism.

The implementation can be easily extended to work with the output of other first-principles codes and will prove more useful once QuantumEspresso implements the calculation of symmetry matrices for systems with non-colinear magnetism and spin-orbit coupling.
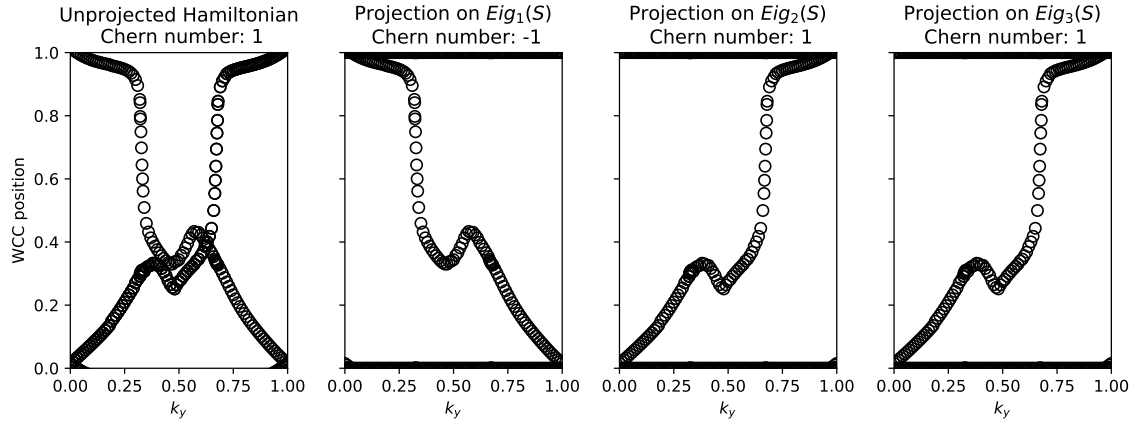
Figure 4.1: Wannier charge centers of block-diagonal Haldane model. The WCCs of the unprojected Hamiltonian are a superposition of the individual WCCs. This is due to the block-diagonal nature of the Hamiltonian in this example. In general, the WCCs of the unprojected system may be divided up in non-trivial ways.

References

[1] D. Gresch *et al.*, "Z2Pack: Numerical implementation of hybrid Wannier centers for identifying topological materials", Phys. Rev. B **95**, 1 (2017).

[2] P. D. Olmsted, *Lectures on Landau Theory of Phase Transitions* (University of Leeds, 2000).

[3] B. A. Bernevig and T. L. Hughes, *Topological insulators and topological superconductors* (Princeton University Press, 2013).

[4] M. Nakahara, *Geometry, Topology and Physics* (IOP Publishing, 2003).

[5] A. A. Soluyanov and D. Vanderbilt, "Computing topological invariants without inversion symmetry", Phys. Rev. B **83**, 1 (2011).

[6] A. A. Soluyanov and D. Vanderbilt, "Smooth gauge for topological insulators", Phys. Rev. B **85**, 115415 (2012).

[7] P. Lochak and C. Meunier, The Quantum Adiabatic Theorem. In: *Multiphase Averaging for Classical Systems* (Springer, 1988), pp. 249–268.

[8] M. Z. Hasan and C. L. Kane, "Colloquium: Topological insulators", Rev. Mod. Phys. **82**, 3045 (2010).

[9] G. H. Wannier, "The Structure of Electronic Excitation Levels in Insulating Crystals", Phys. Rev. **52**, 191 (1937).

[10] N. Marzari and D. Vanderbilt, "Maximally localized generalized Wannier functions for composite energy bands", Phys. Rev. B **56**, 12847 (1997).

[11] N. Marzari, A. A. Mostofi, J. R. Yates, I. Souza, and D. Vanderbilt, "Maximally localized Wannier functions: Theory and applications", Rev. Mod. Phys. **84**, 1419 (2012).

[12] R. D. King-Smith and D. Vanderbilt, "Theory of polarization of crystalline solids", Phys. Rev. B **47**, 1651 (1993).

[13] M. V. Berry, "Quantal Phase Factors Accompanying Adiabatic Changes", Proc. Royal Soc. A: Math. Phys. Eng. Sci. **392**, 45 (1984).

[14] J. Zak, "Berry's Phase for Energy Bands in Solids", Phys. Rev. Lett. **62**, 2747 (1989).

[15] R. Yu, X. L. Qi, A. Bernevig, Z. Fang, and X. Dai, "Equivalent expression of Z2 topological invariant for band insulators using the non-Abelian Berry connection", Phys. Rev. B **84**, 1 (2011).

[16] A. A. Soluyanov, *Topological aspects of band theory*, PhD thesis, 2012.

[17] J. J. Sakurai, *Modern Quantum Mechanics* (Addison-Wesley, 1994).

[18] J. E. Moore and L. Balents, "Topological invariants of time-reversal-invariant band structures", Phys. Rev. B **75**, 1 (2007).

[19] P. Giannozzi *et al.*, "QUANTUM ESPRESSO: a modular and open-source software project for quantum simulations of materials", J. Physics: Condens. Matter **21**, 395502 (2009).

[20] P. Giannozzi *et al.*, "Advanced capabilities for materials modelling with Quantum ESPRESSO", J. Physics: Condens. Matter **29**, 465901 (2017).

[21] R. Sakuma, "Symmetry-adapted Wannier functions in the maximal localization procedure", Phys. Rev. B **87** (2013).

[22] wannier90 : User Guide.

[23] F. D. M. Haldane, "Model for a Quantum Hall Effect without Landau Levels: Condensed-Matter Realization of the "Parity Anomaly"", Phys. Rev. Lett. **61**, 2015 (1988).